Title
Magnetic anisotropy and magnetodielectric coefficients in Cr_2O_3 and $Fe_{0.4}Cr_{1.6}O_3$

Authors
Banerjee, I
Kim, Hyungsuk KD
Pisani, D
et al.

Publication Date
2014-11-01

DOI
10.1016/j.jallcom.2014.06.038

Peer reviewed

Journal of Alloys and Compounds 614 (2014) 305–309

Contents lists available at ScienceDirect

Journal of Alloys and Compounds

journal homepage: www.elsevier.com/locate/jalcom

Magnetic anisotropy and magnetodielectric coefficients in Cr_2O_3 and $Fe_{0.4}Cr_{1.6}O_3$

I. Banerjee [a,b,*], Hyungsuk K.D. Kim [c], D. Pisani [a], K.P. Mohanchandra [a], Gregory P. Carman [a]

[a] Department of Mechanical and Aerospace Engineering, University of California, Los Angeles, CA 90095, USA
[b] Department of Applied Physics, Birla Institute of Technology, Mesra, Ranchi 835215, India
[c] Department of Materials Science and Engineering, University of California, Los Angeles, CA 90095, USA

ARTICLE INFO

Article history:
Received 18 December 2013
Received in revised form 6 June 2014
Accepted 6 June 2014
Available online 18 June 2014

Keywords:
Cr_2O_3
$Fe_{0.4}Cr_{1.6}O_3$
Magnetic anisotropy
Magnetodielectric

ABSTRACT

The temperature dependence of magnetization, magnetic anisotropy, coercive field and the magnetodielectric coefficient of Cr_2O_3 (undoped) and $Fe_{0.4}Cr_{1.6}O_3$ (doped) was experimentally investigated. Test data shows that the presence of Fe ions at the interstitial spaces of the Cr_2O_3 crystal lattice decreases the Neel Temperature by ~80 K when compared to the undoped Cr_2O_3. Also both the doped and undoped samples display maxima in magnetic anisotropy and magnetodielectric coefficient as a function of temperature. The maxima for the Fe doped samples occurs at a temperature approximately 80 K below the temperature measured for the Cr_2O_3 samples, i.e. similar to the shift observed in the Neel Temperature. These results suggest that Neel Temperature, magnetic anisotropy, and the magnetodielectric coefficients are physically interrelated through competing principal exchange interactions and may provide a useful approach to search for new multiferroic materials.

1. Introduction

Discovering a new single phase multiferroic material with the co-existence of large magnetization and polarization coupling has been a scientific endeavor since the early efforts of Curie in 1894. Multiferroicity is generally defined as the coupling between different ferroic orders (electric, magnetic, or elastic) with one subset producing the magnetoelectric effects (ME) and/or the other magnetodielectric effect (MD) [1,2]. While a few single phase materials exhibit ME/MD behavior [3–6], a fundamental understanding of the intrinsic coupling mechanisms is insufficient to adequately search for new materials with large coupling at room temperature. Therefore, understanding ME or MD coefficients and their relationships to other intrinsic material properties is important. Researchers previously believed that ME/MD is maximized at magnetic transition temperatures; however, recent experimental reports and first principle calculations indicated maximum values at temperatures below magnetic transition temperatures [7–12]. While interesting, a clear explanation for this maximum has not been provided and if a correlation could be found with other intrinsic material properties this information may be useful in searching for new MD/ME materials. In this paper we correlate experimentally measured maxima in MD coefficients with maxima in magnetic anisotropy (K_{eff}) coefficients for both Cr_2O_3 and $Fe_{0.4}Cr_{1.6}O_3$.

Both α-Fe_2O_3 and Cr_2O_3 are crystallographic isomorphs stabilized into a rhombohedral corundum structure with space group R3c but with different magnetic ordering [13]. Cr_2O_3 is a well understood ME material system first predicted by Dzyaloshnskii and measured by Astrov in 1961 [14,15]. Cr_2O_3 is a symmetric insulator with low magnetic moment and low antiferromagnetic ordering temperature i.e. Neel Temperature (T_N = 310 K). Researchers have suggested that the magneto electric/magnetoelastic effect in Cr_2O_3 is attributed to changes in magnetic space group symmetry [16]. The magnetic space group symmetry is altered by diffusion/substitution of atoms with similar radius but different magnetic properties such as combining Fe_2O_3 (T_N = 950 K) with Cr_2O_3 yielding $Fe_{2-x}Cr_xO_3$ [17–20]. Such substitution is believed to alter the compressive and tensile stress in the material [18] which influences magnetoelastic coupling. Recent neutron diffraction studies on $Fe_{2-x}Cr_xO_3$ series report a reduction in the Neel temperature T_N, with values ranging from 230 K to 250 K as compared to both Cr_2O_3 ($T_N \sim 310$ K) and Fe_2O_3 with $T_N \sim 950$ K [13,20,21]. While the magnetic structure of the solid solution at $0 < x < 0.6$, where $x = Cr/(Cr + Fe)$, is similar to that of hematite, a different unidentified magnetic ordering involving Fe(III) ions is present in the solid solution $x = 0.8$ below its Néel Temperature

* Corresponding author at: Department of Applied Physics, Birla Institute of Technology, Mesra, Ranchi 835215, India. Tel.: +91 6512275402; fax: +91 6512275401.
E-mail address: indranibanerjee@bitmesra.ac.in (I. Banerjee).

http://dx.doi.org/10.1016/j.jallcom.2014.06.038
0925-8388/

(about 150 K) [22]. This is rather interesting since such magnetic ordering at much lower temperatures than T_N influences the material's magnetic and electrical response. While previous studies evaluated $Fe_{2-x}Cr_xO_3$ alloys magnetic properties [17,18,20,21], reports on the relationship between the MD coefficients with their magnetic properties and/or temperature dependence is unavailable. The present paper attempts to establish a correlation between measured maxima of the effective magnetic anisotropy and magnetodielectric coefficient as a function of temperature for Cr_2O_3 and $Fe_{0.4}Cr_{1.6}O_3$ solid solution.

2. Experimental details

In this paper a solid solution of $Fe_{0.4}Cr_{1.6}O_3$ was fabricated by mechanical alloying of high purity (99.99%) nano crystals of Fe_2O_3 (~15 nm) with Cr_2O_3 (~ 60 nm). Stoichiometric amounts of both materials (Alpha Aesar, USA and Aldrich chemicals) were mechanically ground for 2 h in atmosphere followed by ball milling for ~72 h. Sample dry milling was conducted in air with a 1:7 mass ratio of the materials to zirconia balls. Composite samples were fabricated and the magnetodielectric properties were measured. The composites were prepared by mixing nano powders of either Cr_2O_3 (undoped) or $Fe_{2-x}Cr_xO_3$ (doped) with an epoxy resin (Spurr resin, Polysciences Inc.) at a volume ratio of 50:50. The liquid resin with particles was ultrasonically mixed followed by curing at 70 °C for 12 h. The nanocomposites consisted of densely packed particles producing magnetic coupling between adjacent particles, i.e. dipole–dipole interaction was present. Samples were cut into 3.3 mm × 3.3 mm × 1 mm blocks with silver epoxy electrodes applied along both 3.3 × 3.3 mm^2 areas.

Fourier Transform Infra Ray Spectroscopy (FTIR) was conducted to evaluate the chemical bond formation in both Cr_2O_3 and Fe substituted Cr_2O_3 systems. Micro Raman spectroscopy tests provided information on the magnetic ordering present at room temperature in Cr_2O_3 after Fe substitution. Composites' magnetization measurements at different temperatures along with Zero Field Cooling curves at 50 Oe were also measured using a Superconducting Quantum Interference Device (SQUID, Quantum Design, MPMS XL-5). Dielectric constants were measured using an HP 4274A multi frequency (0–100 kHz) LCR meter with excitation of 1 V and temperature varied from 100 to 300 K at DC magnetic field bias of 1T monitored by a Gauss meter (FW Bell 6010) to evaluate MD as a function of temperature. In the following paragraphs a brief review of the test data generated is provided.

3. Results and discussion

A Scanning Electron Microscope (SEM) image of the $Fe_{0.4}Cr_{1.6}O_3$ powder is shown in Fig. 1. Tests were conducted on both doped and undoped particles as well as composite samples. X-ray diffraction tests were conducted for both doped and undoped composites samples (see Fig. 2). Fig. 2 shows the XRD spectra for Fe_2O_3, Cr_2O_3 and the solid solution powder of $Fe_{0.6}Cr_{1.4}O_3$. The peaks match well the reported spectra [18,23]. The peaks of Fe_2O_3 and Cr_2O_3 phases are well separated before mechanical alloying. However, in the

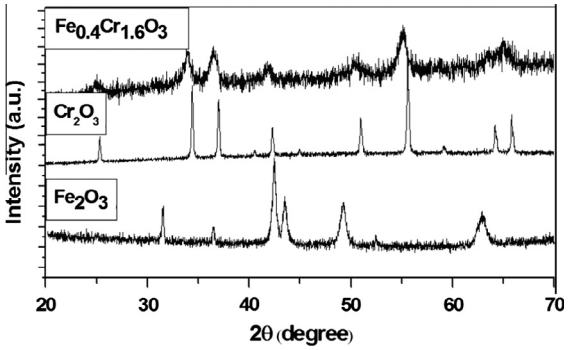

Fig. 2. XRD spectrum for Fe_2O_3, Cr_2O_3 and $Fe_{0.4}Cr_{1.6}O_3$ samples.

$Fe_{0.6}Cr_{1.4}O_3$ solid solution powder the individual peaks of Fe_2O_3 sample disappear and the broader peaks resemble the peaks corresponding to Cr_2O_3. This suggests Fe atoms diffuse into the Cr lattice sites to form a solid solution of $Fe_{0.6}Cr_{1.4}O_3$. The alloy formation involves the kinetic diffusion of Fe^{3+} ions into the boundary of Cr^{3+} ions due to thermal heating during the milling process [2,4,18]. The overall lattice structure of the $Fe_{0.6}Cr_{1.4}O_3$ solid solution consists of Cr_2O_3 having a fraction of Fe^{3+} ions occupying interstitial spaces.

Fig. 3 shows the FTIR spectra for both Cr_2O_3 and $Fe_{0.4}Cr_{1.6}O_3$ nano particles for the wave number 300–2000 cm^{-1}. The merging of the doublet at 581.57 and 635.1 cm^{-1} in the Cr_2O_3 sample into a single broad band in the $Fe_{0.4}Cr_{1.6}O_3$ sample suggests the Fe (III) is being substituted for Cr in the base structure of Cr_2O_3. This indicates a solid solution of $Fe_{0.4}Cr_{1.6}O_3$ nano particles is present rather than a collection of Cr_2O_3 and Fe_2O_3 particles [24].

Fig. 4 shows the Raman spectra recorded at room temperature for both Cr_2O_3 and $Fe_{0.4}Cr_{1.6}O_3$ nano particles. The Raman modes for the Cr_2O_3 sample occur at 338.46 cm^{-1} (E_g), 540.46 cm^{-1} (A_g) and 599.26 cm^{-1} (E_g) [25]. The strongest peak for both samples is observed at 540.46 cm^{-1}. For the $Fe_{0.4}Cr_{1.6}O_3$ sample a broad band extending from 578 to 800 cm^{-1} with a band head at ~675 cm^{-1} is observed. A similar band has also been previously reported in thermally (400 °C) oxidized Cr_2O_3 with $FeCrO_3$ [25,26]. The authors attribute this band to magnon peak representing the energy associated with the collective excitation of the electron spin and anisotropy interactions in the crystal lattice [25]. The presence of this strong magnon peak reduces the spontaneous magnetization and also the temperature dependent magnetic transitions caused due

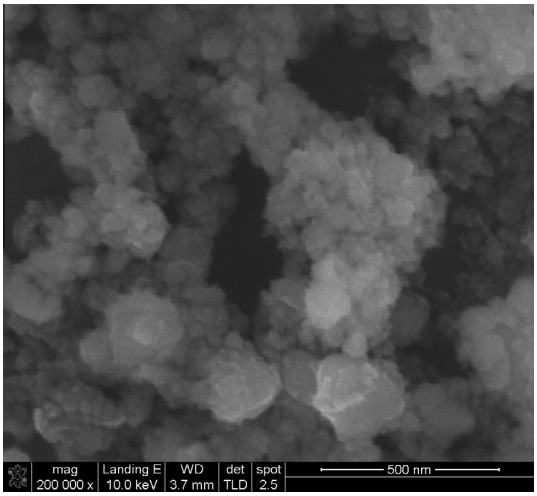

Fig. 1. SEM micrograph of $Fe_{0.4}Cr_{1.6}O_3$ solid solution powder after milling.

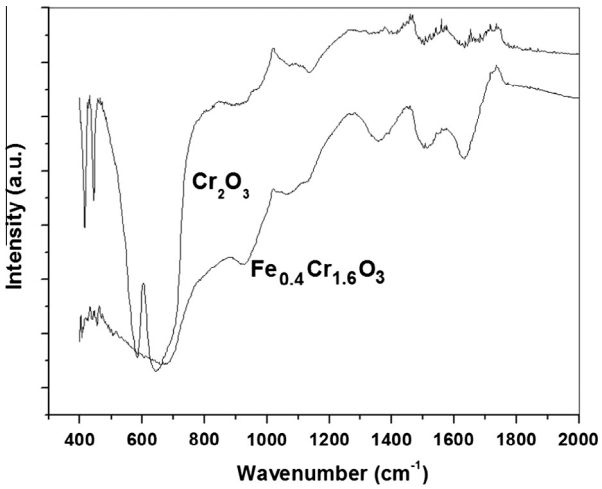

Fig. 3. (a) FTIR spectrum for undoped (Cr_2O_3) and (b) doped ($Fe_{0.4}Cr_{1.6}O_3$) sample.

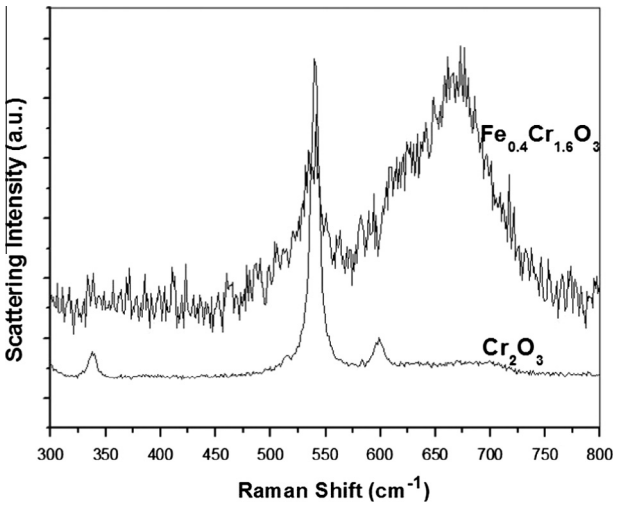

Fig. 4. (a) Raman spectrum at room temperature of the undoped (Cr_2O_3) and (b) doped ($Fe_{0.4}Cr_{1.6}O_3$) sample.

to the presence of Fe^{3+} ions at the interstitial spaces of the Cr_2O_3 crystal lattice in the $Fe_{0.4}Cr_{1.6}O_3$.

Fig. 5 shows a summary of SQUID magnetic measurement results performed on Cr_2O_3 (undoped) and $Fe_{0.4}Cr_{1.6}O_3$ (doped) nanocomposites. Fig. 5(a) displays the magnetization measurements as a function of magnetic field for five different temperatures. As can be seen in Fig. 5(a), the magnetic moment for the doped sample is larger than the undoped sample at all temperatures which is attributed to intrinsically larger magnetic moments associated with Fe. Moreover, the doped sample exhibits larger variation of magnetic moments with temperature as compared to the undoped sample, a feature attributed to the reduction in T_N when Fe is added into the lattice $Fe_{0.4}Cr_{1.6}O_3$ structure.

Fig. 5(b) shows zero-field cooled (ZFC) magnetizations measured for the doped and undoped composite samples. Results show that the T_N for undoped Cr_2O_3 sample is ~310 K, while the T_N for the doped $Fe_{0.4}Cr_{1.6}O_3$ sample is ~230 K. The data is in good agreement with earlier reports [13,20] which also report a decrease in T_N when Fe is added. The $\Delta T \sim 80$ K shift in T_N is attributed to competing principal exchange interactions Γ_a and Γ_b between Cr_2O_3 and Fe_2O_3. The corundum structure of Cr_2O_3 is based on hexagonal close packed array of O^{2-} ions at 18e Wykoff site with 2/3 of the interstitial octahedral sites positioned by Cr^{3+} cations (12c Wykoff site) [13]. The spin moments of $Cr^{3+}(3d^3)$ ions in Cr_2O_3 are arranged in four sublattices out of which two sublattices containing the cations form a ferromagnetic network characterized by an interaction exchange parameter Γ_a. The other two sublattices are coupled antiparallel by the interaction exchange parameter Γ_b [13]. In Cr_2O_3, Γ_a is positive and Γ_b is negative. However, the exchange interactions in Cr_2O_3–Fe_2O_3 system is modified because Fe_2O_3 has both negative Γ_a and Γ_b [13,21]. Therefore the magnetic transition temperature of the solid solution system of Cr_2O_3–Fe_2O_3 reduces with additions of Fe_2O_3 [13]. The Neel Temperature reduction is also indicative of the magnon peak in the doped sample at room temperature (see Raman spectra in Fig. 4).

Fig. 5(c) plots the average coercivities (H_c) as a function of temperature for both doped and undoped samples. The data shows H_c decreases as temperature increases in both samples. The H_c of undoped sample varies from 240 to 140 Oe, whereas H_c for the doped sample varies from 140 to 80 Oe. The smaller H_c for the doped sample is attributed to the diffusion of Fe atoms into the interstitial spaces of Cr_2O_3 crystal lattice representing a hybrid response between Fe_2O_3 and Cr_2O_3 particles. The measured value of H_c for the Fe_2O_3 particles used in the present work is ~70 Oe at 100 K which is contrasted with Cr_2O_3 of 240 Oe at 100 K and a blocking temperature of 310 K.

Fig. 5(d) plots the exchange bias field H_{EB} as a function of temperature for the doped $Fe_{0.4}Cr_{1.6}O_3$ sample. The exchange bias field

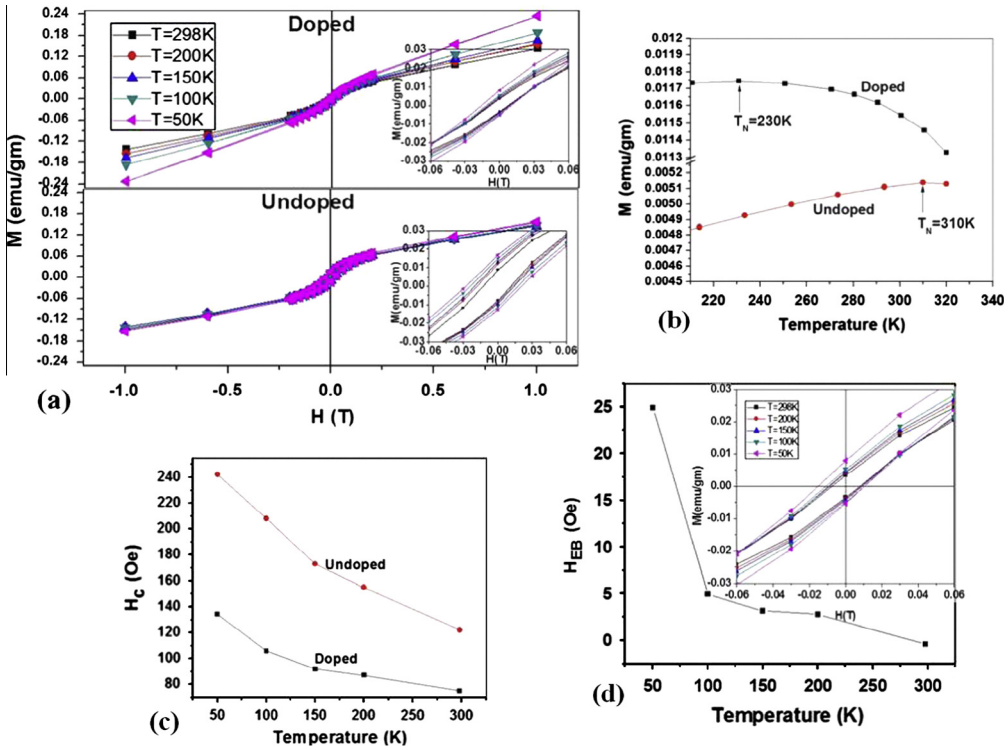

Fig. 5. (a) M–H curves for the nanocomposite at five different temperatures, (b) ZFC curve of the composites representing the $T_N \sim 230$ K for doped ($Fe_{0.4}Cr_{1.6}O_3$) and T_N at ~310 K for undoped (Cr_2O_3) nanocomposites, (c) variation of coercivities with temperature for doped ($Fe_{0.4}Cr_{1.6}O_3$) and undoped (Cr_2O_3) nanocomposites and (d) temperature dependence of exchange bias field (H_{EB}) as a function of temperature for $Fe_{0.4}Cr_{1.6}O_3$ nanocomposite.

H_{EB} is determined from the asymmetric magnetization loops for the doped sample as measured from the magnified view of the M–H curves shown in the inset of Fig. 5d. The magnified M–H curve reveals the existence of antiferromagnetic structure superimposed with weak ferromagnetism for both doped and undoped samples. The weak ferromagnetism results from the partial spin canted moments in the system along with spin–orbit coupling mechanism [13]. The asymmetric magnetization loops for the doped sample shifts towards negative magnetic field values. The exchange bias field is defined as $H_{EB} = -(H_r + H_l)/2$, where H_r and H_l are the coercive field values on the right and left branches of the M–H loops, respectively [27]. As can be seen, the H_{EB} for the doped sample has relatively large values for temperatures $T \ll T_N$ and vanishes near T_N. This implies that the ferro (Fe) and antiferromagnetic (Cr) exchange coupling is pronounced at $T \ll T_N$.

Fig. 6(a) plots the effective magnetic anisotropy coefficient (K_{eff}) as a function of temperature for both composites (note different scale on *Y*-axis). The effective anisotropy coefficient is given by the standard expression as $K_{eff} = 0.5\ (H_a M_s)$ where the effective magnetic anisotropy field (H_a) values have been extracted from the squid data for the M–H plot of Fig. 3(a) [28]. The saturation magnetization M_s was determined by extrapolating the (M–H) curves corrected to (M–χH,H), where χ is determined from M–H curves at high fields ($H \gg H_c$) [20,29]. Fig. 6(a) shows that the undoped sample has a maximum in K_{eff} (1.8×10^6 J/m^3) at ~230 K with values decreasing above this temperature. The K_{eff} magnitude is in good agreement with other reported values for Cr_2O_3 [30–33] but these other reports do not study temperature variations and thus do not report a maximum in K_{eff}. Fig. 6(a) shows that the doped $Fe_{0.4}Cr_{1.6}O_3$ sample also has a maximum $K_{eff} = 0.7 \times 10^6$ J/m^3 but at a lower temperature ~150 K. The K_{eff} maximum for the doped sample is approximately $\Delta T \sim 80$ K lower than the undoped sample. This is important because the temperature shift is almost similar/identical to the temperature shift observed in T_N, (see Fig. 5(b)). When comparing the K_{eff} magnitude between the doped and undoped samples, the undoped sample is 2–3 times larger than the doped sample. Fe doping causes a decrease in the anisotropy field (H_a) which in turn decreases the K_{eff} of the doped sample.

The observed relationship between magnetic anisotropy shifts, and T_N shifts shown in Figs. 6(a) and Fig. 5(b) may be explained with the aid of previous studies and the discussion of principal exchange interactions. Cox et al. attributed the magnetic susceptibility (χ) shifts observed in Fe doped Cr_2O_3 directly to shifts in T_N values [13]. Considering Cox's report coupled with the present observations, it is inferred that the observed shift in K_{eff}, maximum i.e. Fig. 5(a), are directly related to the shift in T_N (Fig. 5(b)) and thus may be related to the same physical phenomenon (i.e. competing principal exchange interactions Γ_a and Γ_b). A discussion on the competing principal exchange interactions was previously provided in the discussion of Fig. 5b.

Fig. 6(b) plots magnetodielectric (MD) as a function of temperature measured at 100 kHz with a DC magnetic field bias of 1*T* for both composites. The MD% is defined as $\frac{\varepsilon(H)-\varepsilon(0)}{\varepsilon(0)} \times$, ($\varepsilon$ = *dielectric constant*). The undoped MD% is relatively constant between 100 and 180 K but increases to a maximum of ~2.2% at ~230 K followed by a decrease up to T_N. Spaldin and Liu recently reported similar analytical results for magnetoelectric coefficients on Cr_2O_3 with maximum values predicted near 230 K [9,11]. Fig. 6(b) shows that the doped MD% also has a maximum (i.e. ~3%) but at a lower temperature 150 K when compared to the undoped sample (230 K). Importantly, the corresponding downward temperature shift in the maximum of MD% is $\Delta T \sim 80$ K which is again similar/identical to the shifts observed in both T_N and K_{eff} values for these two material systems. Furthermore, the maxima in MD% for doped and undoped sample occurs at the same temperature as the measured K_{eff} maximum value shown in Fig. 6(a). Here it is important to point that the relative broadening of the maxima is attributed to particle size distribution within the composites, i.e. not one specific particle size as shown in Fig 1. illustrates the particle size range. Furthermore, the samples have a fairly inhomogeneous particle distribution which also contributes to the broadening of the maxima. Nonetheless, the downward shift of the maxima is clearly visible and the error is well within 10%. These test data strongly suggests that a physical relation exists between the MD coefficient, the effective magnetic anisotropy coefficient, and the T_N values in these samples.

In general, the magnetodielectric properties of a material are attributed either to magneto-resistance or to the changes in electric polarization (ME effect) in the material [3–6,11]. Researchers recently reported that the MD% maximum as a function of temperature corresponds to maximum in effective magnetic anisotropy coefficient of Fe_2O_3 nanocomposites which are not magnetoelectric [33]. However, since Cr_2O_3 is a multiferroic material, the measured MD effect in Fig. 6(b) may arise either due to the magnetoelectric coupling or to both the magnetoresistance and ME coupling. A discussion on this issue follows in the next paragraph.

The MD response for the doped and undoped samples is related to the spin–orbit tunneling across neighboring atoms. On the other hand, the ME response for these materials is due to the physical

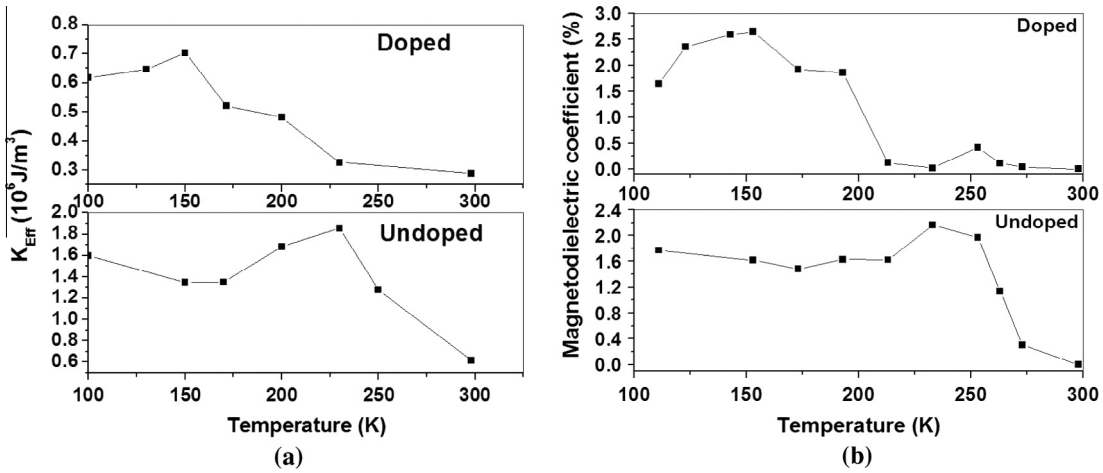

Fig. 6. (a) Effective magnetic anisotropy coefficient (K_{eff}) as a function of temperature for doped ($Fe_{0.4}Cr_{1.6}O_3$) and undoped (Cr_2O_3) nanocomposites and (b) magnetodielectric (MD) coefficient as a function of temperature measured at 100 kHz frequency and at DC magnetic field bias of 1*T* for doped ($Fe_{0.4}Cr_{1.6}O_3$) and undoped (Cr_2O_3) nanocomposites.

coupling between electric polarizations and magnetic dipoles. Doped and undoped Cr_2O_3 consists of antiferromagnetically coupled spin dimers with cone spiral structure. Recent theoretical reports reveal that the overlap of the electron wave function between the neighboring atomic sites with canted spins generates electronic polarization via spin–orbit–interaction [30]. Spontaneous spin-current flows between mutually canted spin sites through spin orbit tunneling mechanism (origin of MD effect). Analogous to the charge current producing magnetic field, the spin current also generates a "fictitious" electric field and electric polarization [30]. This spin mechanism causes the microscopic origin of the linear magnetoelectric effect ($P = \alpha H$) perpendicular to *c*-axis of the corundum structure in Cr_2O_3 and $Fe_{0.4}Cr_{1.6}O_3$ [30]. Therefore, the correlation of the maximum MD% and $K_{eff.}$ at the same temperature may be explained with the following hypotheses which are supported by earlier reports [30]. We postulate that K_{eff} is maximum when either the spin orbit coupling is maximum for magneto resistive materials or the coupling between magnetic and electric dipoles is maximum for magnetoelectric materials, which takes an additional energy to reorient both the magnetic and electric dipoles from the easy axis. As observed from Raman spectrum (Fig. 4), the origin of magnon peak in $Fe_{0.4}Cr_{1.6}O_3$ shows the existence of magnetic surface spins at room temperature which contributes to its magnetic ordering. As explained earlier, the percentage of Fe(III) in the solid solution controls the magnetic properties at different temperatures. The resultant magnetic structure for the solid solution is determined by the competing exchange interaction parameters of Γ_a and Γ_b. A long range continuous magnetic order has been reported for this solid solution which retains a cone spiral structure with simple antiferromagnetic ordering similar to Cr_2O_3 [13]. Any change in composition is accommodated by a change in the spiral periodicity and cone geometry, while retaining identical crystal structure [13,18,31]. The magnetic ordering in the $Fe_{0.4}Cr_{1.6}O_3$ solid solution has also been reported using Mossbauer spectroscopy at different temperatures [22]. Literature reveals that or $x = 0.8$, where $x = Cr/(Cr + Fe)$, i.e. $Fe_{0.4}Cr_{1.6}O_3$, an unidentified magnetic ordering sets in at ~150 K [22]. This has been explained by the establishment of Fe–O–Cr superexchange leading to the best possible coordination of the neighboring spins, i.e. maximum effective magnetic anisotropy. However, the decrease in anisotropy further below 150 K could be due to thermal agitation disturbing the spin alignment. Recent reports suggest that the maximum in magnetic dipole alignment for magnetoresistive materials corresponds to maxima in magneto dielectric coefficient as well as effective magneto crystalline anisotropy coefficient [34]. Now since Cr_2O_3 is a multiferroic, the maximum in MD coefficient and magnetic dipole alignment i.e. effective magnetic anisotropy could be expected to arise due to magnetoelectric coupling phenomenon also. Further studies that directly measure the ME coefficient need to be performed to confirm the correlation with the ME coefficients as observed for the MD coefficients in this manuscript. If this hypothesis is correct it provides another tool for better understanding of multiferroics and may provide an avenue to both search for new material and/or design new single phase materials with superior coupling.

4. Conclusions

The magnetic properties of Cr_2O_3 and $Fe_{0.4}Cr_{1.6}O_3$ nano particles have been investigated for wide range of temperature and applied magnetic field. Test results show that a maximum in the MD% correlates with a maximum in the effective magnetic anisotropy which is also related to shifts in T_N. It is speculated that future optimization of magnetic anisotropy may lead to improved MD/ME coupling in single phase multiferroic materials.

Acknowledgement

The authors would like to acknowledge financial support from a MURI program by the Air Force Office of Scientific Research managed by Byung-lip (Les) Lee contract number FA9550-09-1-0677. The author I. Banerjee wants to acknowledge Department of Science and Technology (DST), Government of India for financial support of BOYSCAST programme (SR/BY/E-04/10) under which the work was performed.

References

[1] J. Hemberger, P. Lukenheimer, R. Fichtl, H.-A. Krug von Nidda, V. Tsurkan, A. Loidl, Nature 434 (2005) 364–367.
[2] .N. Hur, S. Park, P.A. Sharma, J.S. Ahn, S. Guha, S.-W. Cheong, Nature 429 (2004) 392–395.
[3] G. Catalan, Appl. Phys. Lett. 88 (2006) 1029021–1029023.
[4] G. Lawes, R. Tackett, O. Masala, B. Adhikary, R. Naik, R. Seshadri, Appl. Phys. Lett. 88 (2006) 2429031–2429033.
[5] H.H.B. Rocha, F.N.A. Freire, R.R. Silva, D.X. Gouveia, J.M. Sasaki, M.R.P. Santos, J.C. Goes, A.S.B. Sombra, J. Alloys Comp. 481 (2009) 438–445.
[6] Y.S. Koo, T. Bonaedy, K.D. Sung, J.H. Jung, J.B. Yoon, Y.H. Jo, M.H. Jung, H.J. Lee, T.Y. Koo, Y.H. Jeong, Appl. Phys. Lett. 91 (2007) 2129031–2129033.
[7] T. Kimura, S. Kawamoto, I. Yamada, M. Azuma, M. Takano, Y. Tokura, Phys. Rev. B 67 (2003) 1804011–1804014.
[8] T. Bonaedy, Y.S. Koo, K.D. Sung, J.H. Jung, Appl. Phys. Lett. 91 (2007) 1329011–1329013.
[9] Y.Y. Liu, S.H. Xie, G. Jin, J.Y. Li, J. Appl. Phys. 105 (2009) 0739171–0739175.
[10] J. Cao, R.C. Rai, S. Brown, J.L. Musfeldt, R. Tackett, G. Lawes, Y.J. Wang, X. Wei, M. Apostu, R. Suryanarayan, A. Revcolevschi, Appl. Phys. Lett. 91 (2007) 0219131–0219133.
[11] Maxim Mostovoy, Andrea Scaramucci, Nicola A. Spaldin, Kris T. Delaney, Phys. Rev. Lett. 105 (2010) 0872021–0872024.
[12] D.L. Hou, X.F. Nie, H.L. Luo, Appl. Phys. A 66 (1998) 109–114.
[13] D.E. Cox, W.J. Takei, G. Shirane, J. Phys. Chem. Solids 24 (1963) 405–423.
[14] E. Dzyaloshinskii, Sov. Phys. JEPT 10 (1959) 628–629.
[15] D.N. Astrov, Solv. Phys. JEPT 13 (1961) 729–733.
[16] S. Di Matteo, C.R. Natoli, Phys. Rev. B 66 (2002) 2124131–2124134.
[17] Kiran Singh, Antoine Maignan, Charles Simon, Christine Martin, Appl. Phys. Lett. 99 (2011) 1729031–1729033.
[18] R.N. Bhowmik, M. Nrisimha Murty, E. Sekhar Srinadhu, PMC Phys. B I (2008) 201–218.
[19] S. Ali Jawad, S.Z. Ashrafi, J. Alloys Comp. 599 (2013) 13–21.
[20] E. Loughiri, A Belayachi, M. Nogues, M. Taibi, A. Dahmani, M.EL. Yamani, J. Aride, M. J. Condens. Mat. 31 (2000) 98–105.
[21] Z. Latacz, M. Baster, J. Alloys Comp. 464 (2008) 23–27.
[22] Tomas Grygar, Petr Bezdicka, Jiri Dedecek, Eduard Petrovsky, Oldrich Schneeweiss, Ceramics-Silikáty 47 (1) (2003) 32–39.
[23] Nitin Kaduba Chaudhari, Hyoung Chan Kim, Derac Son, Jong-Sung Yu, Cryst. Eng. Commun. 11 (2009) 2264–2267.
[24] Yang Xiaojuan, Chen Naiseng, Shen Suifa, Liu Ersheng, Huang Jinling, Sci. China Ser. B 41 (4) (1998) 442–448.
[25] Robert Baco Arroya, Miguel Galvan Arellano, Gabriel R. Paredes Rubio, Ramon Pena Sierra, Lecture notes in Information Technology, in: 2nd International Conference on Materials, Mechatronics and Automation, 2012, pp. 140–145.
[26] M.I. Baraton, G. Busca, M.C. Prieto, G. Ricchiardi, V. Sanchez Escribano, J. Solid State Chem. 112 (1994) 9–14.
[27] T. Ambrose, R.L. Sommer, C.L. Chien, Phys. Rev. B 56 (1) (1997) 83–86.
[28] N.A. Frey, S.S. Srinath, H. Srikanth, Phys. Rev. B 74 (2006) 0244201–0244208.
[29] Manuel Banobre-Lopez, Carlos Vazquez-Vazquez, Jose Rivas, M. Arturo Lopez-Quintela, Nanotechnology 14 (2003) 318–322.
[30] Yoshinori Tokura, Shinichiro Seki, Adv. Mater. 22 (2010) 1554–1565.
[31] G.P. Vorob'ev, A.M. Kadomtseva, A.S. Moskvin, Yu.F. Popov, V.A. Timofeeva, Phys. Solid State 39 (1) (1997) 97–98.
[32] D. Tobia, E. Winkler, R.D. Zysler, M. Granada, H.E. Troiani, D. Fiorani, J. Appl. Phys. 106 (2009) 1039201–1039206.
[33] D. Tobia, E. De Biasi, M. Granada, H.E. Troiani, G. Zampieri, E. Winkler, D. Zysler, J. Appl. Phys. 108 (2010) 1043031–1043038.
[34] I. Banerjee, H.S. Kim, K.P. Mohanchandra, Scott Keller, Greg Carman, IEEE Magn. Lett. 4 (2013) 25001041–25001045.